



HAL
open science

Overcoming the thermal stability limit of chalcogenide Phase-Change Materials for high-Temperature applications in $\text{GeSe}_{1-x}\text{Te}_x$ thin films

Martina Tomelleri, Françoise Hippert, Thierry Farjot, Christophe Licitra, Nicolas Vaxelaire, Jean-Baptiste Dory, Daniel Benoit, Valentina Giordano, Pierre Noé

► To cite this version:

Martina Tomelleri, Françoise Hippert, Thierry Farjot, Christophe Licitra, Nicolas Vaxelaire, et al.. Overcoming the thermal stability limit of chalcogenide Phase-Change Materials for high-Temperature applications in $\text{GeSe}_{1-x}\text{Te}_x$ thin films. *physica status solidi (RRL) - Rapid Research Letters*, 2020, 15, pp.2000451. 10.1002/pssr.202000451 . hal-03037216

HAL Id: hal-03037216

<https://hal.science/hal-03037216>

Submitted on 2 Nov 2021

HAL is a multi-disciplinary open access archive for the deposit and dissemination of scientific research documents, whether they are published or not. The documents may come from teaching and research institutions in France or abroad, or from public or private research centers.

L'archive ouverte pluridisciplinaire **HAL**, est destinée au dépôt et à la diffusion de documents scientifiques de niveau recherche, publiés ou non, émanant des établissements d'enseignement et de recherche français ou étrangers, des laboratoires publics ou privés.

Overcoming the Thermal Stability Limit of Chalcogenide Phase-Change Materials for High-Temperature Applications in GeSe_{1-x}Te_x Thin Films

*Martina Tomelleri, Françoise Hippert, Thierry Farjot, Christophe Licitra, Nicolas Vaxelaire, Jean-Baptiste Dory, Daniel Benoit, Valentina Giordano and Pierre Noé**

Ms. Martina Tomelleri, Mr. Thierry Farjot, Mr. Christophe Licitra, Dr. Nicolas Vaxelaire, Dr. Jean-Baptiste Dory, Dr. Pierre Noé

Univ. Grenoble Alpes, CEA, LETI, F-38000, Grenoble, France.

*E-mail: pierre.noe@cea.fr

Prof. Françoise Hippert

Univ. Grenoble Alpes, CNRS, Grenoble INP, LMGP, F-38000 Grenoble, France.

Ms. Martina Tomelleri, Dr. Daniel Benoit
STMICROELECTRONICS, F-38920 Crolles, France.

Dr. Valentina Giordano

ILM, UMR 5306 Univ. Lyon 1-CNRS, F-69622 Villeurbanne Cedex, France.

Keywords: chalcogenide, GeSeTe, thermal stability, phase-change memories, metavalent bonding

Abstract

Herein, the electrical, optical and structural properties of GeSe_{1-x}Te_x phase-change materials thin films with $0.16 \leq x \leq 1$ prepared by co-sputtering of GeSe and GeTe targets are studied. The crystallization temperature of the films increases significantly when the Te content decreases. Se-rich films show an extremely large electrical contrast between their amorphous and crystalline states. A high polarizability of the crystalline phase is observed in the entire x range and is related to the presence of metavalent bonds. This is explained by the persistence of a rhombohedral crystalline phase, isostructural to GeTe, in the GeSe_{1-x}Te_x films down to $x = 0.16$. Hence, the substitution of only 16 at % of the Se atoms by Te atoms transforms covalent GeSe into a phase-change material with a huge and unprecedented contrast of resistivity (up to 11 orders of magnitude) and a very high thermal stability (up to 10 years at 272°C) for an alloy exhibiting no phase separation upon crystallization. This outstanding combination of properties

makes Se-rich $\text{GeSe}_{1-x}\text{Te}_x$ thin films extremely promising for integration in memory devices requiring a very high data retention such as automotive and embedded applications.

The integration of chalcogenide Phase-Change Materials (PCMs) in non-volatile resistive memories is currently attracting a great deal of interest.^[1, 2, 3] PCMs, such as alloys belonging to the GeTe-Sb₂Te₃ pseudo-binary line in the ternary Ge-Sb-Te phase diagram, exhibit fast and reversible phase transformations between their amorphous (a-) and crystalline (c-) states. The large electrical and optical contrast between the a- and c- phases has been ascribed to the existence of a particular bonding mechanism in the crystalline state. This bonding mechanism, first depicted as resonance bonding,^[4] was recently redefined as “MetaValent” Bonding (MVB)^[5] since it is in fact fundamentally different from the resonant bonding in materials such as benzene or graphite. MVB mechanism can be described as in between covalent and metallic bonding but it is none of that. It explains the high electronic conductivity of the PCM crystalline phase (several order of magnitude higher than that of the insulating amorphous one) and its high electronic polarizability, leading to its high optical dielectric constant and is thus also at origin of the optical contrast between the amorphous and crystalline states of PCMs. Moreover, MVB results in a high chemical bond polarizability evidenced by unusually high Born effective charges, as well as uncommon vibrational properties such as unusual phonon softening and large Grüneisen parameters.^[5]

Thanks to their unique properties, PCMs have enabled the development of the most promising resistive memory technology, especially after their successful integration above a chalcogenide ovonic threshold switching (OTS) glass selector in a 3D cross point architecture.^[6-9] Despite their multi-level storage capability, high endurance, high programming speed and scalability,^[1,3, 10-13] PCM memories still have technological limits to overcome for large-scale integration. In particular, for embedded applications, the code integrity must be guaranteed for 10 years at 150°C, as well as during the soldering reflow process (a few min at 260°C) for final memory chip packaging.^[14, 15] The data retention time of the memory is directly related to the thermal stability of the a-phase against unwanted crystallization. The most common approach so far has been to use Ge-Sb-Te alloys enriched in Ge with respect to alloys on the GeTe-Sb₂Te₃

pseudo-binary line. The crystallization of these Ge-rich alloys is slowed down thanks to the required out-diffusion of Ge excess from the PCM grains.^[16] In thin films with an optimized composition, called “T-alloy” with “Theta composition”,^[15-17] the crystallization occurs at 360°C, to be compared to 150-170°C in the prototypical Ge₂Sb₂Te₅ alloy thin films.^[1] Nevertheless, the Ge phase segregation upon crystallization is difficult to master and can lead to integration non-reproducibility issues in devices, hindering the programming of the memory cell. Here the need to find new PCMs with high thermal stability but with very limited or no phase separation. In the present study, we show that some alloys belonging to the GeSe-GeTe pseudo-binary line in the Ge-Se-Te ternary phase diagram meet these requirements and provide in addition an extremely large electrical contrast, unprecedented among the phase-change materials studied so far.

GeTe is a prototypical PCM.^[1] Amorphous GeTe crystallizes in a rhombohedral structure in which the Ge atom has a distorted octahedral environment with an intermediate degree of Peierls distortion allowing the formation of metavalent Ge-Te bonds.^[5] GeSe is a covalently bonded material^[5] with a low resistivity contrast between the a- and c-states.^[18] The phase diagram of GeSe_{1-x}Te_x bulk polycrystals, made by alloying the elements at high temperature, was studied and three different crystalline structures were identified at room temperature.^[19, 20] A rhombohedral phase, isostructural to GeTe, is observed for $0.48 \leq x \leq 1$ and an orthorhombic phase, isostructural to GeSe, for $0 \leq x \leq 0.08$. For x between 0.14 and 0.42, a hexagonal structure is observed. The atomic structure of the GeSe_{0.75}Te_{0.25} hexagonal phase has been recently determined.^[21] The electronic properties of GeSe_{1-x}Te_x alloys were little studied in the literature until recently in thin films for memory application^[18, 22] and in bulk polycrystals for thermoelectric applications.^[23]

In this work, we investigate the electronic, optical and structural properties of GeSe_{1-x}Te_x thin films with $0.16 \leq x \leq 1$ and compare them to those of GeSe and GeTe films. Amorphous films

were deposited at room temperature by co-sputtering using GeSe and GeTe targets (see the **Experimental Section**). Their crystallization was observed by measuring their resistivity and optical properties during annealing.

Figure 1 shows the resistivity of $\text{GeSe}_{1-x}\text{Te}_x$ thin films as a function of temperature. Upon heating the crystallization leads to a large drop in resistivity. The crystallization temperature T_x of the $\text{GeSe}_{1-x}\text{Te}_x$ films, defined as the maximum of the derivative of the resistivity curve, increases strongly when the Te concentration decreases. T_x is already 100°C higher than for GeTe when x is equal to 0.86 and reaches $\sim 350^\circ\text{C}$ for $x = 0.16$. It is worth mentioning that all the films are protected against surface oxidation. The crystallization temperature of the GeTe reference film is 215°C (instead of 180°C for an oxidized GeTe film).^[24, 25] In the a-state, the resistivity shows a semi-conducting behavior for all x values. Moreover, at a given temperature, the resistivity of amorphous film decreases strongly with x : from $\sim 10^8 \Omega\cdot\text{cm}$ in a-GeSe to $\sim 10^6 \Omega\cdot\text{cm}$ when x is equal to 0.36 and down to $\sim 10^3 \Omega\cdot\text{cm}$ in a-GeTe at 50°C . The resistivity of the crystalline state is almost independent of temperature for x between 0.16 and 0.86. It increases only slightly when the Te concentration decreases, remaining of the order of its value in the GeTe film ($\sim 10^{-3} \Omega\cdot\text{cm}$). As a result, the resistivity contrast between the a- and c-phases increases considerably when the Te concentration decreases, reaching 11 orders of magnitude at 50°C in the film with a Te concentration of 8 at % ($x = 0.16$). By contrast, in the GeSe film, a semi-conducting behavior is observed in both the a- and c-states and the resistivity of the two states differs by less than four orders of magnitude at 50°C . A slight resistivity drop is detected in the crystallized state at 317°C in GeTe and at higher temperature in $\text{GeSe}_{1-x}\text{Te}_x$ films (except for GeSe), for instance at 380°C for $x = 0.36$. It is due to the crystallization of some germanium in excess (see x-ray diffraction data in the **Supporting Information**). Besides, for all x values between 0.16 and 0.86, a change of the slope of the resistivity curve is observed when heating at a temperature (denoted T_s) about 50°C before the sharp resistivity drop. Between T_s and the

temperature of the resistivity drop, the resistivity remains high, but lower than expected by extrapolation of its behavior from 50°C to T_s . This change of slope is not present in GeTe.

Isothermal resistivity measurements on $\text{GeSe}_{1-x}\text{Te}_x$ thin films were also carried out at several fixed temperatures as a function of time (see the **Supporting Information**). From these, one can estimate the temperature at which the a-phase is stable for 10 years: 245°C for $x = 0.36$ and 272°C for $x = 0.16$. The expected data retention largely meets the industrial criteria for embedded and automotive applications and for the soldering reflow of a few minutes at 260°C.^[15, 26]

The outstanding electrical contrast observed in $\text{GeSe}_{1-x}\text{Te}_x$ films is mainly due to the low resistivity of their pseudo-metallic crystalline state, similar to that of the GeTe alloy, even for a low Te content down to $x = 0.16$. By analogy with GeTe, this observation could be due to the presence of MVB in the crystalline state and to the very high electronic polarizability of Ge-Te bonds by contrast with the significantly less polarizable covalent Ge-Se bonds of the semiconducting GeSe compound.^[5, 27] To confirm this interpretation, the study of the real part of the optical dielectric constant is a key tool. For this purpose, the amorphous $\text{GeSe}_{1-x}\text{Te}_x$ films deposited on Si were crystallized by annealing up to 400°C at a heating ramp of 10°C min⁻¹ and then cooling down to room temperature. The dielectric constant ϵ_r was deduced from the modelling of spectroscopic ellipsometry (SE) data in the wavelength range [190-1700 nm] (see the **Supporting Information**). Except in the case of GeSe, the ϵ_r values in the c- and a-films differ strongly, as shown in **Figure 2** for a wavelength of 1700 nm. In the a-phase, ϵ_r at 1700 nm is close to ϵ_∞ but this is not the case for the c-phase (see the **Supporting Information**). Hence, in the following we compare the values of ϵ_r at 1700 nm, which is the maximum wavelength of the experimental set-up. ϵ_r is high in all crystallized $\text{GeSe}_{1-x}\text{Te}_x$ films with x varying between 0.16 and 1. The highest value ($\epsilon_r = 45$) is measured in crystalline GeTe. ϵ_r

slightly decreases when x decreases reaching a value of 27.5 for $x = 0.16$. The latter is significantly higher than the ϵ_r value of 15 reported in crystalline GeSe.^[28]

In summary, a concentration of only 8 at % of Te ($x = 0.16$) atoms in GeSe_{1-x}Te_x films leads to a dramatic decrease of the resistivity in the crystalline state with respect to the case of GeSe, correlated to a marked increase of the dielectric constant. This striking result shows that MVB is present in crystallized GeSe_{1-x}Te_x thin films at least down to $x = 0.16$, which was totally unexpected given the structural studies reported so far in literature.^[19,21] We show below that it is due to the fact that the crystallized phase in the thin films has a rhombohedral structure.

In the case of the film with $x = 0.22$, representative of the behavior of all GeSe_{1-x}Te_x films with x between 0.16 and 0.86, we also studied the change of optical properties during heating up to 425°C at a heating rate of 10°C min⁻¹ by means of an in situ SE experiment. The resistivity, previously presented in Figure 1, and Ψ the amplitude of the complex reflectance ratio measured by SE at a wavelength of 1097 nm are shown as a function of increasing temperature in **Figure 3**. The transition from a- to c-phase marked by the resistivity drop is accompanied by an increase of Ψ . The temperature at which the optical and electrical properties change abruptly is nearly the same. The slight difference of 5°C can result from a slight composition difference between the studied samples (film deposited on SiO₂ for the resistivity and on Si for SE) and from experimental uncertainties on the sample temperature. It should also be noted that the two techniques do not probe the same kind of properties and a slight mismatch between the optical and the electrical change is possible. By modelling the in situ SE data at different wavelengths, since the penetration depth of the incoming light is higher than the film thickness in the near infrared region, one can conclude that the entire thickness of the film is probed. Therefore, the whole film shows the same optical behaviour as a function of temperature and hence the same crystallization process.

The change in the slope of the resistivity that occurs at $T_s = 300^\circ\text{C}$ coincides with a small increase of Ψ . These changes could reflect a change of the amorphous structure accompanied by a change of its electronic density of states (DoS). They could also be ascribed to thermally activated electronic transport mechanisms, such as Poole-Frenkel type conduction, as expected in amorphous chalcogenides.^[3, 29] However, the correlation between optical and electrical changes could rather suggest the formation of crystalline nuclei within the majority amorphous covalent network at a temperature (T_s) smaller than T_x which corresponds to the abrupt crystallization of the whole film. A link between optical and electrical behavior is also observed after crystallization. An abrupt change of Ψ occurs at the temperature of the minor drop in the resistivity curve that corresponds to the crystallization of Ge in excess.

In order to get insight on the origin of the outstanding properties of the $\text{GeSe}_{1-x}\text{Te}_x$ films, we have investigated by x-ray diffraction (XRD) at room temperature the structure of films crystallized by heating at 400°C . Selected parts of the XRD patterns are shown in **Figure 4a** and **4b**. The full XRD patterns are given in the **Supporting Information**. The main result is that a rhombohedral structure is observed for all films in the x range [0.16-1] (Peak indexation in Figure 4a and 4b uses a hexagonal unit cell to describe the rhombohedral structure). The existence of a doublet of two close diffraction peaks in the 2θ range [41-46°] is a direct consequence of the rhombohedral distortion. XRD measurements at varying tilt angle in the range [0-70°] on films with $x = 0.16$ and $x = 0.22$ confirm the absence of other crystalline Ge-Se-Te phase in the annealed films. Besides, in agreement with literature results, the crystallized GeSe film has an orthorhombic structure (see the **Supporting Information**).^[20, 30] The presence of a small amount of crystallized Ge is detected in most films, as expected from the resistivity curves (Figure 1). In summary, the crystallization of amorphous $\text{GeSe}_{1-x}\text{Te}_x$ thin films leads to a rhombohedral phase from $x = 1$ down to $x = 0.16$. This is surprising because in $\text{GeSe}_{1-x}\text{Te}_x$ bulk polycrystals the domain of existence of the rhombohedral phase is limited to the x range [0.48-1] and an hexagonal phase is observed for x between 0.42 and 0.14 and a mixture of

hexagonal and rhombohedral phases for $0.42 < x < 0.48$.^[19] The existence of a metastable rhombohedral structure in $\text{GeSe}_{1-x}\text{Te}_x$ thin films with x values from 0.44 to 0.16, explains their high dielectric constant and low electrical resistivity, as discussed below. The studied films have been crystallized by heating the initially amorphous film up to 400°C with a ramp of $10^\circ\text{C min}^{-1}$ and cooling down at the same rate. Annealing the films for longer time and/or at higher temperature probably leads to the transformation of the metastable rhombohedral phase into the stable hexagonal one. This point deserves further studies. Nevertheless, we can expect that in memory devices, where changes of states are induced by short current pulses, amorphous $\text{GeSe}_{1-x}\text{Te}_x$ with x values from 0.44 to 0.16 will transform into the metastable (rhombohedral) phase, as it is the case with the prototypical $\text{Ge}_2\text{Sb}_2\text{Te}_5$ alloy, which switches between the amorphous phase and a metastable (*fcc*) phase.

A progressive shift of all diffraction peaks to higher angles is observed as x decreases in Figure 4a and 4b, as well as a progressive increase in the separation of the two peaks of the doublet. This reveals a continuous change of the lattice parameters of the rhombohedral phase with x . The rhombohedral GeTe phase (space group *R3m*) can be described as a distorted cubic structure (see the **Supporting Information**). The pseudo-cubic unit cell of GeTe (which contains 4 Ge and 4 Te atoms) is a rhombohedron (edge a_c) with an angle α_c slightly less than 90° .^[31] Using this description for crystallized $\text{GeSe}_{1-x}\text{Te}_x$ films, we determined the a_c and α_c values and the pseudo-cubic unit cell volume V_c . Both a_c and V_c continuously increase with x over the range [0.16-1] (**Figures 4c and 4d**). For $x \geq 0.48$, the values of a_c and V_c in crystallized films are in close agreement with those measured on rhombohedral $\text{GeSe}_{1-x}\text{Te}_x$ bulk polycrystals,^[19, 20, 23] In ref. [19], the changes of a_c and V_c with x in bulk polycrystals with $x \geq 0.48$ were fitted by linear laws. Thanks to the extension of the existence domain of the rhombohedral phase in thin films, we observe that the same trends continue down to $x = 0.16$. This typical solid solution effect can be ascribed to the progressive replacement of Te atoms (covalent radius = 1.35 \AA) by smaller Se atoms (covalent radius 1.17 \AA) in the rhombohedral

structure.^[19] For x values between 0.44 and 0.16, the volume of the pseudo-cubic unit cell in the metastable rhombohedral phase is smaller than the volume of the unit cell of the stable hexagonal phase^[19, 21] (Figure 4d).

α_c decreases with decreasing x (**Figure 4e**). This trend is responsible for the progressive increase of the angular separation between the two diffraction peaks of the doublet when x decreases (Figure 4b). The fact that α_c drifts away from 90° when x decreases reveals an increasing distortion of the pseudo-cubic structure. In GeTe, this behavior occurs when the temperature decreases and it is correlated with a continuous change of the position of the Ge atom, as determined by diffraction.^[31] In the present case, no information on the atom positions in the unit cell can be extracted from XRD patterns of GeSe_{1-x}Te_x thin films. In Figures 4a and 4b, one notes that the relative integrated intensities of the peaks vary a lot with x but the effect of structure factors on peak intensities cannot be separated from texture effects. These latter are indeed present in the films and they depend on x . The α_c values measured in crystallized GeSe_{1-x}Te_x thin films are found systematically higher than those measured in bulk polycrystals. This observation also applies to GeTe (see the discussion in the **Supporting Information**). From the width of the diffraction peak measured in the 2θ range [29-32°], one can estimate an average grain size. It varies between 22 and 47 nm with no clear trend as a function of x (see the **Supporting Information**).

The rhombohedral structure of crystallized GeSe_{1-x}Te_x films would explain the existence of polarizable metavalent bonds, at the origin of their uncommon high optical dielectric constant. Although crystalline GeSe and GeTe are isoelectronic compounds with six p -electrons available for bonding, their structure significantly differs. GeTe has a rhombohedral structure and exhibits a moderate Peierls distortion, characterized by three short and three long bonds. The formation of MVB in GeTe is favored by an optimal degree of distortion, which reduces the coupling between p -orbitals and enables a kind of resonance, which is at the origin of MVB.^[5]

^{18,27]} By contrast, the strong distortion of orthorhombic GeSe breaks down MVB and crystalline GeSe is covalently bonded (as demonstrated by the limited electrical contrast between its a- and c-phases). Although the deviation of α_c from 90° increases with decreasing Te content (Figure 4e), the increasing Peierls distortion still satisfies the conditions for the formation of MVB, even for Se-rich films down to $x = 0.16$. Thus, the presence of the rhombohedral phase, metastable for x between 0.16 and 0.48 allows MVB, which instead should not survive in the hexagonal $\text{GeSe}_{1-x}\text{Te}_x$ phase,^[32, 33] stable for this range of compositions. Further studies are under progress for x values between 0.16 and 0 to deeply investigate the transition from MVB to covalent bonding.

Another interesting remark concerns the uncommon change in slope of resistivity at T_s that anticipates the major drop (Figure 1) and seems to be correlated with an increase of Ψ (Figure 3). This behavior, absent in GeTe, could indicate the beginning of nucleation within the amorphous film and the formation of localized MVB structural motifs, due to local p -orbitals alignment inside the amorphous covalent matrix. This may explain the increase of the material polarizability observed in SE as well as the concomitant modification of the electronic DoS, justifying the change in slope of the resistivity curve. However, due to the too small size of MVB crystalline nuclei or MVB motifs that progressively form in the remaining a-phase with increasing temperature, no percolation of the latter can occur in the covalent network until the full film is crystallized. Then, the major resistivity drop corresponds to such percolation and results in the overlapping of electron wave function between the atomic motifs, giving rise to the overall pseudo-metallic behavior of the crystalline $\text{GeSe}_{1-x}\text{Te}_x$ phase with $x \geq 0.16$.

Regarding the programming speed of $\text{GeSe}_{1-x}\text{Te}_x$ compounds, it should first be pointed out that in the advanced GST T-alloy (Ge-rich GST with at least more than 50% Ge!), the huge Ge phase separation required during crystallization tends to increase the switching time considerably (1.5-2 μs for this famous T-alloy) compared to standard phase-change alloys (~ 200 ns for the GST 225 using the same memory cell architecture).^[15] However, this issue

does not prevent the T-alloy from being well suited for embedded memory applications.^[14, 15] In this context, as no or negligible phase separation occurs in $\text{GeSe}_{1-x}\text{Te}_x$ alloys upon crystallization, one can expect that the switching time of these alloys will be compatible for use in embedded PCM memory. Promising preliminary information is available in the literature.^[18] Although the GeSe compound without Te is not expected to be as fast to crystallize and thus to program as GeTe, a switching speed of 500 ns for a cell size of 190 nm has been reported for Se-rich GeSeTe alloys in PCM memory devices.^[18] Since in the same study crystallization in these alloys is shown to follow a growth-dominated crystallization mechanism, the crystallization time can be further reduced by using smaller cell sizes. In summary, we do not foresee any major concern for the use of GeSeTe alloys even for Se-rich compositions for embedded PCM memory applications. Their performance in devices will be the subject of future work.

In conclusion, Se-rich $\text{GeSe}_{1-x}\text{Te}_x$ thin films exhibit an exceptional thermal stability reaching a stability of 272°C for 10 years for $x = 0.16$ while having, thanks to the presence of MVB, a huge electrical contrast between the a- and the c- phase. This outstanding combination of properties in a homogeneous alloy, without occurrence of phase segregation (excluding the presence of a very small amount of crystallized Ge), is unprecedented among all the PCMs materials studied so far, making Se-rich $\text{GeSe}_{1-x}\text{Te}_x$ thin films extremely promising for integration in memory devices. A film containing 37% of Te has been recently integrated in a PCRAM device, showing a data retention of 208°C (crystallization temperature of 262°C).^[18] From the present study, even better performances are expected for alloys with a lower Te content.

Experimental Section

Thin films deposition

GeSe_{1-x}Te_x films were deposited at room temperature by magnetron co-sputtering of GeSe and GeTe pure targets in an industrial cluster tool on silicon substrate (200 mm diameter) under Ar atmosphere. The power applied to the two targets was adjusted in order to deposit amorphous films with x varying from 0 to 1. Film thicknesses were determined by spectroscopic ellipsometry (SE) and found to vary between 75 and 90 nm (see the **Supporting Information**). For each x value, we deposited two sets of films differing by the substrate preparation in order to optimize the stacking for each of the characterization techniques used. A first set, deposited on Si (001) substrate, was used for SE measurements and x-ray diffraction (XRD) experiments. A second set was deposited on 500 nm thick thermal silicon oxide layer obtained by thermal oxidation of a 700 μm thick Si (001) substrate. These films were used for electrical resistivity measurements. After deposition, all the samples were protected by in situ deposition of a 10 nm thick SiN capping layer in order to avoid surface oxidation. The compositions of the as-deposited GeTe and GeSe reference films were determined by WDXRF (Wavelength Dispersive X-ray Fluorescence). They were found close to the nominal ones with a slight excess of Ge of about 1-2 % at in the case of the GeTe film, as usual in GeTe films deposited by sputtering.^[24, 25] The Te concentration in the GeSe_{1-x}Te_x films was determined by WDXRF. Results are given in **Table S5** of the **Supporting Information**. No significant differences between the GeSe_{1-x}Te_x films deposited on Si and SiO₂ is observed, and an average Te concentration is used to label the samples.

Resistivity vs temperature measurements

Four-point probe resistivity measurements were performed as a function of temperature by heating the films of the series deposited on 500 nm thick SiO₂ up to 430°C with a ramp of 10°C min⁻¹ and then cooling to room temperature at the same rate. During the measurements, the

samples were kept in dry atmosphere by showering their surface with a high N₂ gas flow in order to avoid oxidation.

Spectroscopic ellipsometry

SE measurements on the films deposited on Si were performed by using a J. A. Woollam M-2000 equipment operating in the 190-1700 nm range. Room temperature SE data were collected on the amorphous films and on films previously annealed up to 400°C at three incidence angles (55, 65 and 75°). The SE raw data were analysed using WVASE 32® software. For the in situ SE experiment, a dedicated furnace was mounted on the SE setup and data at one incident angle of 70° were collected each ~9-10 s during annealing at 10°C min⁻¹ up to 425°C.

X-ray diffraction experiment (XRD)

The crystalline structure of the films deposited on a Si substrate and annealed at 400°C was studied by XRD at room temperature in Bragg Brentano geometry (*Cu K_α* radiation at 1.542 Å, offset of 3°). We also performed complementary XRD experiments in grazing incidence geometry (incident angle of 1°, *Cu K_α* radiation).

Supporting Information

Supporting Information is available from the author.

Acknowledgements

The authors sincerely acknowledge C. Le Galliard whose master internship was at origin of the first samples allowing the start of the present study. This study has been supported mainly by the bilateral program Alpha between Leti and ST Microelectronics. J.-Y. Raty from FNRS-Liège University in Belgium is also sincerely acknowledged for numbers of fruitful discussions regarding the MVB theory.

References

- [1] P. Noé, C. Vallée, F. Hippert, F. Fillot, J.-Y. Raty, *Semicond. Sci. Technol.* **2018**, *33*, 013002.
- [2] M. Longo, P. Fantini, P. Noé, *J. Phys. D: Appl. Phys.* **2020**, *53*, 440201.
- [3] A. Redaelli, Ed., *Phase Change Memory*, Springer International Publishing, Cham, **2018**.
- [4] a) G. Lucovsky, R. M. White, *Phys. Rev. B* **1973**, *8*, 660; b) J. Robertson, K. Xiong, P. W. Peacock, *Thin Solid Films* **2007**, *515*, 7538; c) K. Shportko, S. Kremers, M. Woda, D. Lencer, J. Robertson, M. Wuttig, *Nature Materials* **2008**, *7*, 653; d) B. Huang, J. Robertson, *Phys. Rev. B* **2010**, *81*, 081204.
- [5] a) M. Wuttig, V. L. Deringer, X. Gonze, C. Bichara, J.-Y. Raty, *Adv. Mater.* **2018**, *30*, 1803777; b) J.-Y. Raty, M. Schumacher, P. Golub, V. L. Deringer, C. Gatti, M. Wuttig, *Adv. Mater.* **2019**, *31*, 1806280.
- [6] J.-Y. Raty, P. Noé, *physica status solidi (RRL) – Rapid Research Letters* **2020**, *14*, 1900581.
- [7] P. Noé, A. Verdy, F. d’Acapito, J.-B. Dory, M. Bernard, G. Navarro, J.-B. Jager, J. Gaudin, J.-Y. Raty, *Sci. Adv.* **2020**, *6*, eaay2830.
- [8] T. Kim, H. Choi, M. Kim, J. Yi, D. Kim, S. Cho, H. Lee, C. Hwang, E. R. Hwang, J. Song, S. Chae, Y. Chun, J. K. Kim, in *2018 Int. Electron Devices Meeting (IEDM)*, IEEE, San Francisco, CA **2019**, 37.1.1.
- [9] J. Choe, Tech Insights Blog, May 2017, <https://www.techinsights.com/blog/intel-3d-xpoint-memory-die-removed-intel-optanetm-pcm-phasechange-memory>.
- [10] S. Raoux, G. W. Burr, M. J. Breitwisch, C. T. Rettner, Y.-C. Chen, R. M. Shelby, M. Salinga, D. Krebs, S.-H. Chen, H.-L. Lung, C. H. Lam, *IBM J. Res. Dev.* **2008**, *52*, 465.
- [11] G. W. Burr, S. Kim, M. Brightsky, A. Sebastian, H.-L. Lung, H.-Y. Cheng, N. E. S. Cortes, J. Y. Wu, H. Pozidis, C. Lam, *IEEE Journal on Emerging and Selected Topics in Circuits and Systems* **2016**, *6*, 146.

- [12] G. W. Burr, *J. Vac. Sci. Technol.* **2010**, B 28, 223.
- [13] R. Bez, A. Pirovano, *Mater. Sci. Semicond. Process.* **2004**, 7, 349.
- [14] P. Fantini, *J. Phys. D: Appl. Phys.* **2020**, 53, 283002.
- [15] P. Cappelletti, R. Annunziata, F. Arnaud, F. Disegni, A. Maurelli, P. Zuliani, *J. Phys. D: Appl. Phys.* **2020**, 53, 193002.
- [16] M. Agati, M. Vallet, S. Joulié, D. Benoit, A. Claverie, *J. Mater. Chem. C.* **2019**, 7, 8720-8729.
- [17] V. Sousa, G. Navarro, N. Castellani, M. Coue, O. Cueto, C. Sabbione, P. Noe, L. Perniola, S. Blonkowski, P. Zuliani, R. Annunziata, *Symp. on VLSI Tech. Dig.* **2015**, T98.
- [18] K. Ren, M. Zhu, W. Song, S. Lv, M. Xia, Y. Wang, Y. Lu, Z. Ji, Z. Song, *Nanoscale* **2019**, 11, 1595.
- [19] H. Wiedemeier, P. A. Siemers, *High Temp. Sci.* **1984**, 17, 395.
- [20] M. G. Herrmann, R. P. Stoffel, M. Küpers, M. Ait Haddouch, A. Eich, K. Glazyrin, A. Grzechnik, R. Dronskowski, K. Friese, *Acta Cryst B* **2019**, 75, 246.
- [21] M. Küpers, P. M. Konze, S. Maintz, S. Steinberg, A. M. Mio, O. Cojocaru-Mirédin, M. Zhu, M. Müller, M. Luysberg, J. Mayer, M. Wuttig, R. Dronskowski, *Angewandte Chemie International Edition* **2017**, 56, 10204.
- [22] E. I. Lee, B.-K. Ju, Y.-T. Kim, *Microelectron. Eng.* **2009**, 86, 1950.
- [23] L. Yang, J. Q. Li, R. Chen, Y. Li, F. S. Liu, W. Q. Ao, *Journal of Elec. Materi.* **2016**, 45, 5533.
- [24] P. Noé, C. Sabbione, N. Bernier, N. Castellani, F. Fillot, F. Hippert, *Acta Materialia* **2016**, 110, 142.
- [25] P. Noé, F. Hippert, in *Phase Change Memory*, Springer, Cham, **2018**, pp. 125-179.
- [26] P. Zuliani, E. Varesi, E. Palumbo, M. Borghi, I. Tortorelli, D. Erbetta, G.D. Libera, N. Pessina, A. Gandolfo, C. Prelini, L. Ravazzi, R. Annunziata, *IEEE Trans. Electron Devices* **2013**, 60, 4020.

- [27] J.-Y. Raty, M. Wuttig, *J. Phys. D: Appl. Phys.* **2020**, *53*, 234002.
- [28] S.-C. Liu, Y. Mi, D.-J. Xue, Y.-X. Chen, C. He, X. Liu, J.-S. Hu, L.-J. Wan, *Adv. El. Mater.* **2017**, *3*, 1700141.
- [29] A. Verdy, G. Navarro, M. Bernard, P. Noe, G. Bourgeois, J. Garrione, M.-C. Cyrille, V. Sousa, E. Nowak, in *2018 IEEE International Memory Workshop (IMW)*, IEEE, **2018**, pp. 1-4.
- [30] H. Wiedemeier, H. G. von Schnering, *Zeitschrift für Kristallographie* **1978**, *148*, 295.
- [31] T. Chattopadhyay, J. X. Boucherle, H. G. von Schnering, *J. Phys. C. Solid State Physics* **1987**, *20*, 1431.
- [32] Y. Yu, M. Cagnoni, O. Cojocaru-Mirédin, M. Wuttig, *Adv. Funct. Mater.* **2020**, *30*, 1904862.
- [33] M. Zhu, O. Cojocaru-Mirédin, A. M. Mio, J. Keutgen, M. Küpers, Y. Yu, J.-Y. Cho, R. Dronskowski, M. Wuttig, *Adv. Mater.* **2018**, *30*, 1706735.

Figures

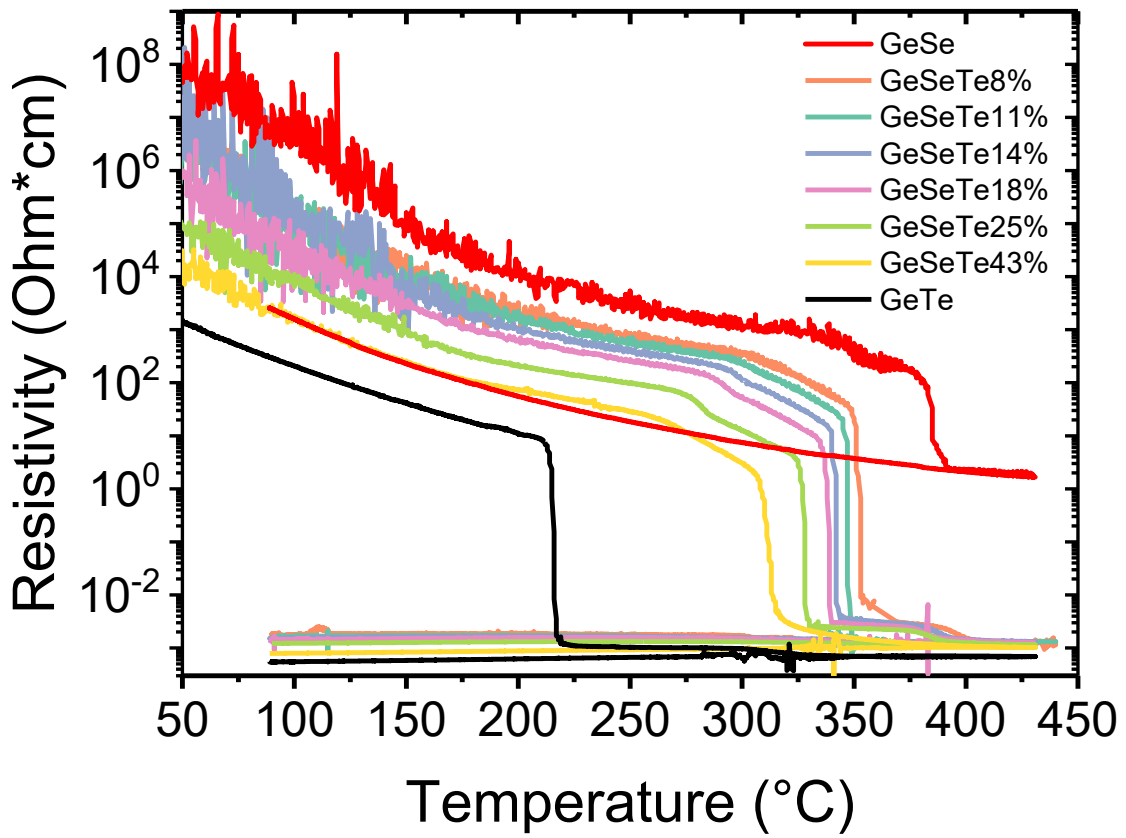


Figure 1. Resistivity of $\text{GeSe}_{1-x}\text{Te}_x$ thin films measured as function of temperature at a heating and cooling rate of $10^\circ\text{C min}^{-1}$. The percentage indicated in the labels is the Te atomic concentration.

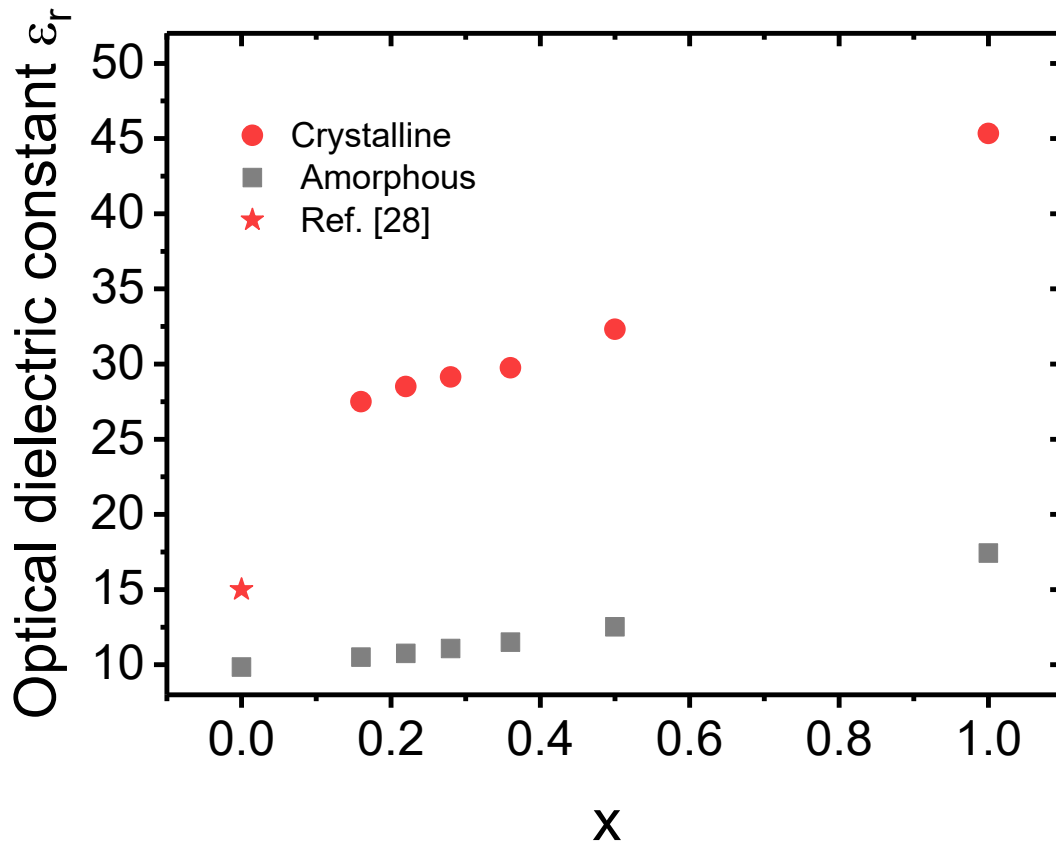


Figure 2. Optical dielectric constant ϵ_r as a function of x measured at room temperature for a wavelength of 1700 nm in $\text{GeSe}_{1-x}\text{Te}_x$ thin films in the amorphous as-deposited state and in the crystallized state obtained after annealing the films up to 400°C. The optical characterization of the crystallized GeSe and $\text{GeSe}_{1-x}\text{Te}_x$ films with $x = 0.72$ and 0.86 was not possible due to a damage of the film surface after annealing hindering thus an accurate SE modelling. The reported value for crystalline GeSe is taken from ref. [28].

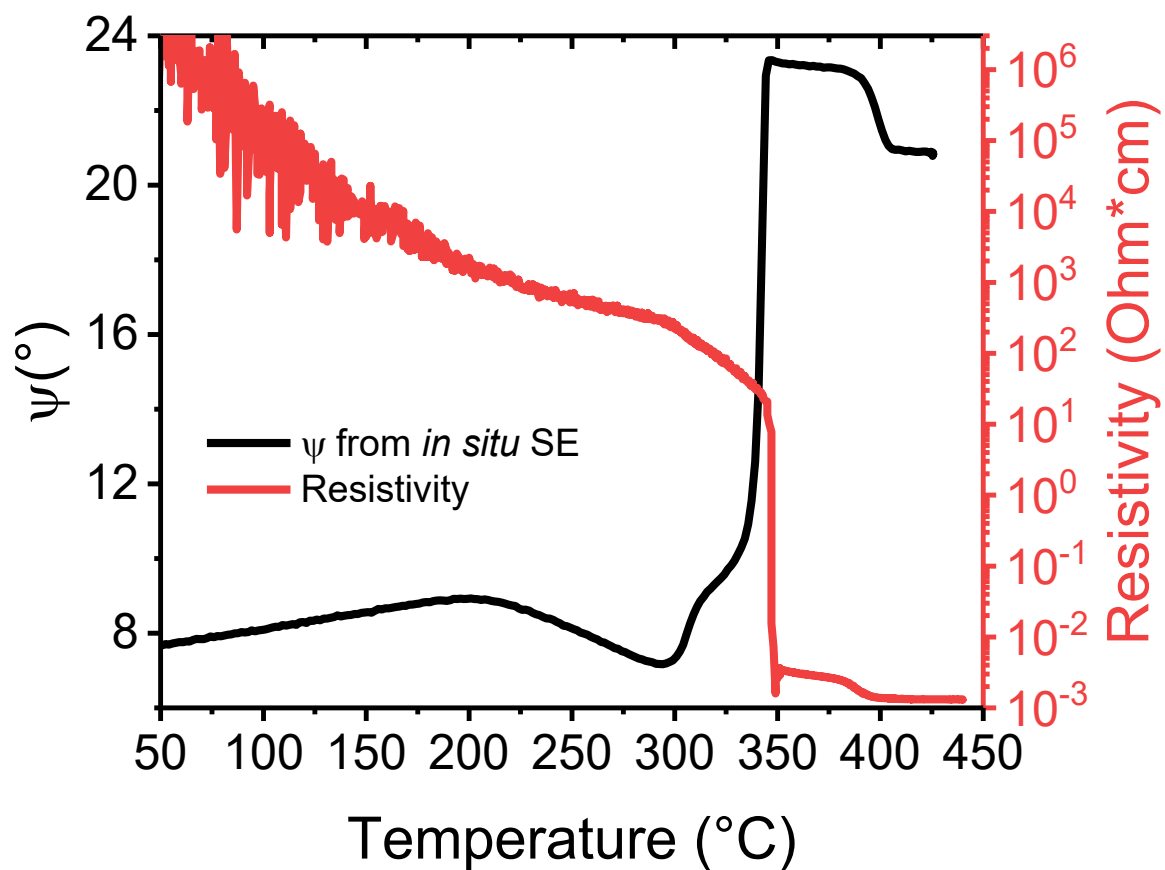


Figure 3. Resistivity (red) and Ψ parameter measured by *in situ* SE (black) as a function of temperature at a heating ramp of $10^{\circ}\text{C min}^{-1}$ for the $\text{GeSe}_{1-x}\text{Te}_x$ film containing 11% of Te ($x = 0.22$).

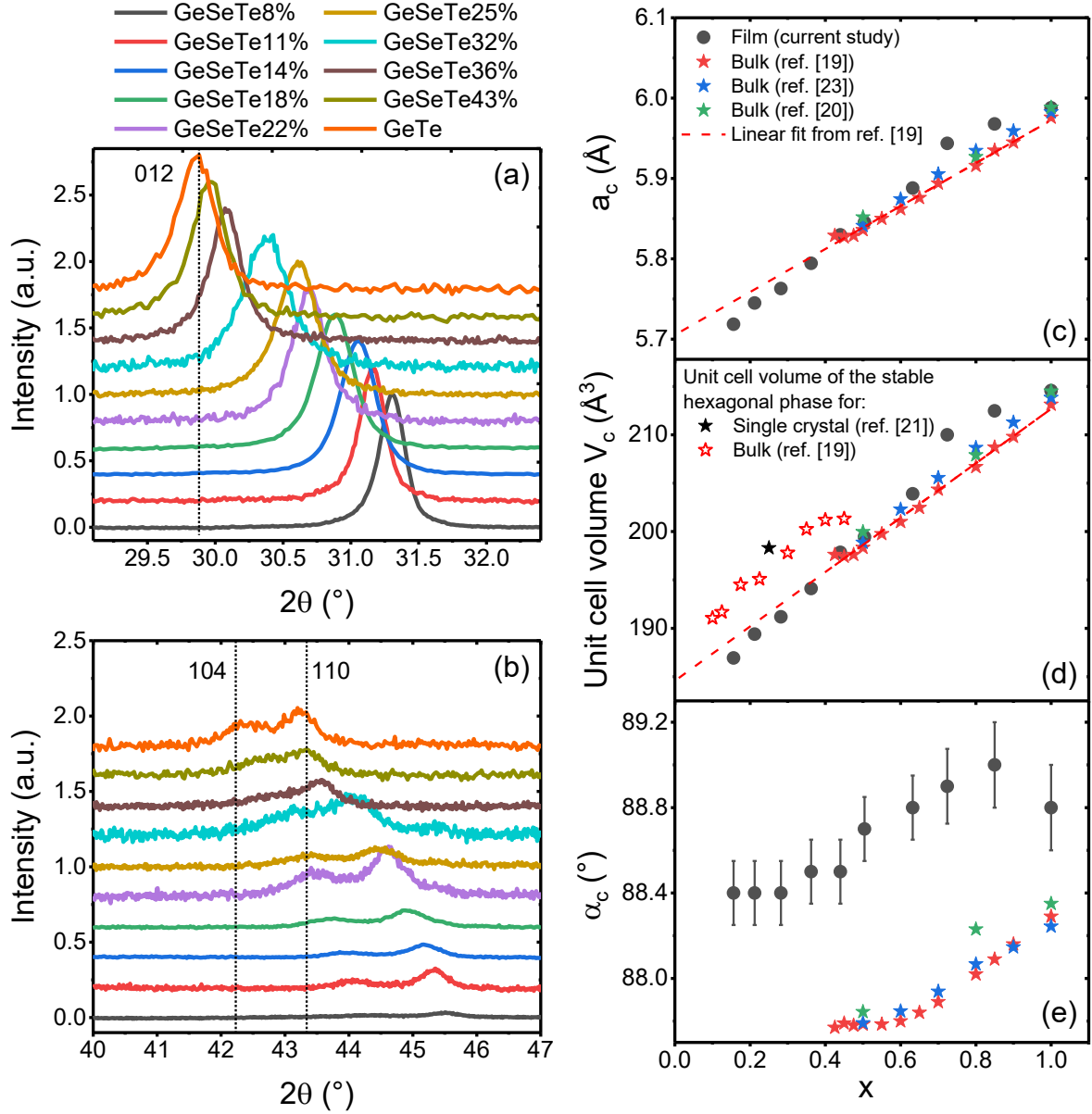


Figure 4. *a, b)* XRD patterns of $\text{GeSe}_{1-x}\text{Te}_x$ thin films crystallized by heating up to 400°C measured in the Bragg-Brentano geometry at room temperature. All films have a rhombohedral structure. The dashed lines indicate the diffraction angles of the (012), (104) and (111) peaks (hexagonal indexing) in GeTe. The spectra have been normalized so that the maximum intensity (for the (012) peak) is set to 1. *c)* Cell edge a_c , *d)* volume V_c and *e)* angle α_c of the pseudo-cubic unit cell as a function of x . In *c)*, *d)* and *e)* values obtained in thin films (circles) are compared with literature results on polycrystalline ingots.^[19, 20, 23] In *d)* the unit cell volume of the stable hexagonal phase for x between 0.1 and 0.45 is also reported.^[19, 21] The dashed lines in *c)* and *d)* are the linear laws accounting for the results of ref. [19]. The error bars on the a_c and V_c values in thin films are smaller than the symbol size.